

Crystallization Behavior of Amorphous Fe-Tb-M (M=Si or Al) Alloys and High Magnetostriction of their Crystallized Phases

著者	Inoue Akihisa, Tanaka Yoshitaka, Miyauchi Yoshihiro, Masumoto Tsuyoshi
journal or publication title	Science reports of the Research Institutes, Tohoku University. Ser. A, Physics, chemistry and metallurgy
volume	39
number	2
page range	147-153
year	1994-03-25
URL	http://hdl.handle.net/10097/28485

Crystallization Behavior of Amorphous Fe-Tb-M (M=Si or Al) Alloys and High Magnetostriction of their Crystallized Phases*

Akihisa Inoue, Yoshitaka Tanaka¹, Yoshihiro Miyauchi¹, and Tsuyoshi Masumoto

Institute for Materials Research, Tohoku University, Sendai 980, Japan

¹*Nippon Denko Co., Ltd., Anan 779-13, Japan*

(Received December 13, 1993)

The addition of 2.5 at% Si or Al to Fe₂Tb causes the formation of an amorphous single phase and the glass formation range extends up to 15 at% Si or Al which is the maximum additional amount in the present study. The amorphous (Fe₂Tb)_{97.5}M_{2.5} (M=Si or Al) alloys crystallize through two stages consisting of Am → Fe₂Tb + Am → Fe₂Tb + unknown compound. The Fe₂Tb phase in coexistent with the amorphous phase has a very fine spherical morphology with a particle size of 5 to 20 nm. The additional Si or Al element is enriched into the unknown compounds. The coexistent state of the nanocrystalline Fe₂Tb and amorphous phases extends over the temperature region of about 300 K because of the high thermal stability of the remaining amorphous phase. The high thermal stability of the amorphous phase and the formation of the nanoscale Fe₂Tb grains are presumably due to the necessity of the redistribution of Si or Al into the remaining amorphous phase. The best magnetostrictive properties of high σ_{1440} , low H_c , high λ_s and high λ/H were obtained in the coexistent nanocrystalline Fe₂Tb and amorphous phases and the phase transition into Fe₂Tb and unknown compounds caused the depression of the magnetostrictive properties.

KEYWORDS: amorphous alloy, rapid solidification, iron-terbium base alloy, nanocrystalline Laves phase, high magnetostriction

1. Introduction

It has been reported in 1976¹⁾ that the low temperature annealing of amorphous alloys in Pd-, Fe-, Ni- and Co-based systems causes the formation of a fine mixed structure consisting of nanoscale metallic particles embedded in the amorphous matrix. By utilizing the nanostructure caused by crystallization, good soft magnetic properties combined with high saturation magnetization have been reported to be obtained in Fe-Si-B-Cu-Nb²⁾, Fe-Ta-C³⁾, Fe-Zr-B⁴⁾ and Fe-Nb-B⁵⁾ systems. The achievement of good soft magnetic properties such as low coercivity and high permeability has been presumed^{2, 4, 5)} to originate from the combination of the following three factors; (1) the disappearance of apparent crystallographic magnetic anisotropy due to the refinement of bcc grains, (2) the maintenance of structural homogeneity resulting from the bcc grain size which is smaller than the size of 180 degree domain walls, and (3) the achievement of a high magnetic coupling state between the nanoscale bcc grains via thin amorphous layer with ferromagnetism.

An Fe₂Tb Laves compound is known to exhibit high magnetostriction, but there is a great disadvantage that the high magnetostriction is obtained only under a high applied magnetic field. Accordingly, a new material exhibiting a high magnetostriction even in a low applied magnetic field has strongly been desired. As one method to overcome the disadvantage, the replacement of Tb by Dy in Fe₂Tb has been reported⁶⁾ to cause the appearance of high magnetostriction in a low applied field, even though the maximum magnitude of magnetostriction decreases significantly. It is reasonable to expect that the nanoscale refinement of the grain size for the Fe₂Tb Laves phase causes the decrease in crystallographic magnetic anisotropy as well as in coercivity, leading to the appearance of high magnetostriction in a low applied field. Although the formation of an amorphous

single phase by melt spinning is very difficult in Fe-Tb binary system, we have found⁷⁾ that the addition of a small amount of Si or Al is very effective for the increase in the glass-forming ability and an amorphous phase is obtained in rather wide composition ranges in Fe-Tb-Si and Fe-Tb-Al systems. Furthermore, the addition of Si or Al is also expected to cause the improvement of the magnetostrictive properties for Fe₂Tb, based on the fact that soft magnetic properties of α -Fe are improved by the dissolution of these elements. The first aim of this paper is to examine the composition ranges in which an amorphous phase is formed in Fe-Tb-Al and Fe-Tb-Si systems by melt spinning, the compositional dependence of their crystallization behavior and the changes in magnetostriction, saturation magnetization and coercivity of the amorphous and crystallized alloys with alloy composition and annealing temperature. The second is to investigate the usefulness of the present alloy design to develop a new-type of magnetostrictive material with high magnetostriction in a low applied field.

2. Experimental

Alloy ingots of Fe₂Tb binary and (Fe₂Tb)_{100-x}Si_x and (Fe₂Tb)_{100-x}Al_x ternary systems were produced by arc melting mixtures of pure Fe, Tb and Al metals and pure Si crystal in an argon atmosphere. The subscripts represent the nominal alloy compositions. Rapidly solidified ribbons with a cross section of about 0.02x1 mm² were produced in an argon atmosphere by a single-roller melt spinning method in which the copper roller with a diameter of about 200 mm is rotated at a circumferential speed of 21 m/s. The as-quenched samples were subjected to heating for 3.6 ks at various temperatures ranging from 673 to 973 K inside a vacuum-sealed quartz tube, followed by air cooling. As-quenched and annealed structures were examined by X-ray diffractometry and transmission electron microscopy (TEM). The decomposition behavior upon continuous heat-

* IMR, Report No. 1957

ing at a rate of 0.17 K/s was also examined by differential scanning calorimetry (DSC), differential thermal analysis (DTA) and X-ray diffractometry. Magnetization (σ) and coercive force (H_c) were measured under an applied field of 1440 kA/m at room temperature with a vibrating sample magnetometer. Magnetostriction was measured at room temperature in an applied field up to 240 kA/m by a three-terminal capacitance method.

3. Results and Discussion

Figure 1 shows the X-ray diffraction patterns of melt-spun $(\text{Fe}_2\text{Tb})_{100-x}\text{Si}_x$ alloys containing 0, 2.5, 7.5 and 15 at% Si. Although the melt-spun Fe_2Tb alloy consists of the rhombohedral Laves phase and no amorphous phase is formed, the increase in Si content to 2.5 % causes the formation of a mostly single amorphous phase. We confirmed that the amorphous single phase formed up to 15 %Si in the melt-spun $(\text{Fe}_2\text{Tb})_{100-x}\text{Si}_x$ alloys. Thus, the addition of a small amount of Si is very effective for the increase in the glass-forming ability of Fe_2Tb alloy. A similar increase in the glass-forming ability is also recognized for melt-spun $(\text{Fe}_2\text{Tb})_{100-x}\text{Al}_x$ alloys. As shown for the X-ray diffraction patterns in Fig. 2, the as-quenched structure changes from the Laves phase to an amorphous phase only by the addition of 2.5 %Al. The glass formation range extends up to about 7.5 %Al. As is evident from Fig. 2, the wave vector at the peak position of the halo pattern due to the formation of the amorphous phase, (K_p), shifts gradually with increasing Al content, indicating that the additional Al element has been dissolved into the amorphous phase.

Figures 3 and 4 show the DSC curves of the amorphous $(\text{Fe}_2\text{Tb})_{100-x}\text{Si}_x$ and $(\text{Fe}_2\text{Tb})_{100-x}\text{Al}_x$ ($x=2.5, 5$ and 7.5 at%) alloys, respectively. It is seen that all the alloys crystallize through two exothermic reactions with each peak at the

temperatures marked with arrows. However, one can notice a significant difference in the temperature ranges of each exothermic reaction between the Fe-Tb-Si and the Fe-Tb-Al alloys. That is, the two exothermic reactions are completely separated for the Fe-Tb-Al alloys while those for the Fe-Tb-Si alloys overlap because of the decrease in the temperature of the second-stage exothermic reaction. Here, it is to be noticed that the first-stage exothermic reaction for the Fe-Tb-Al amorphous alloys takes place over a very wide temperature range from about 570 to 850 K. In order to examine the crystalline phases which precipitate by the two exothermic reactions, Figs. 5 and 6 show the X-ray diffraction patterns of the $(\text{Fe}_2\text{Tb})_{97.5}\text{Si}_{2.5}$ and $(\text{Fe}_2\text{Tb})_{97.5}\text{Al}_{2.5}$ alloys in the as-quenched state and heated to 723 and 823 K, respectively, corresponding to the temperature range of the first exothermic peak and 973 K in the second exothermic peak. The diffraction peaks are identified to be only the Fe_2Tb Laves phase for both samples heated to 723 and 823 K and a mixed structure of the Laves compound and unknown crystalline phase for both samples heated to 973 K. This result indicates that the first broad exothermic peak is due to the precipitation of the Laves phase from the amorphous matrix and the second exothermic peak results from the precipitation of an unknown compound from the remaining amorphous phase. Although the definitely analyzed result on the unknown compound is not obtained, the position of the diffraction peaks corresponding to the unknown compound differs completely between both alloys. Accordingly, the unknown phase seems to be compounds containing Si, as a main constituent element, for the Fe-Tb-Si alloy and Al for the Fe-Tb-Al alloy, though the Si and Al concentrations are much lower as compared with those for Fe and Tb.

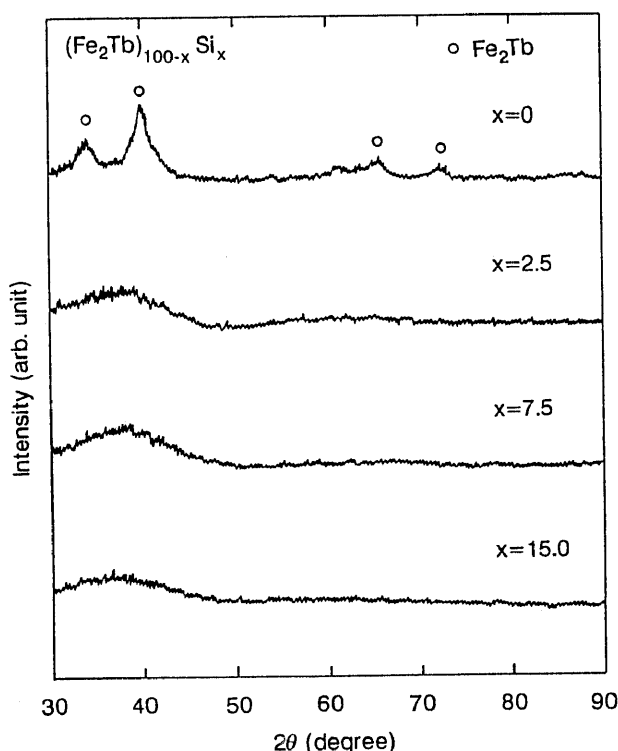


Fig. 1. X-ray diffraction patterns of rapidly solidified $(\text{Fe}_2\text{Tb})_{100-x}\text{Si}_x$ ($x=0, 2.5, 7.5$ and 15 at%) alloys.

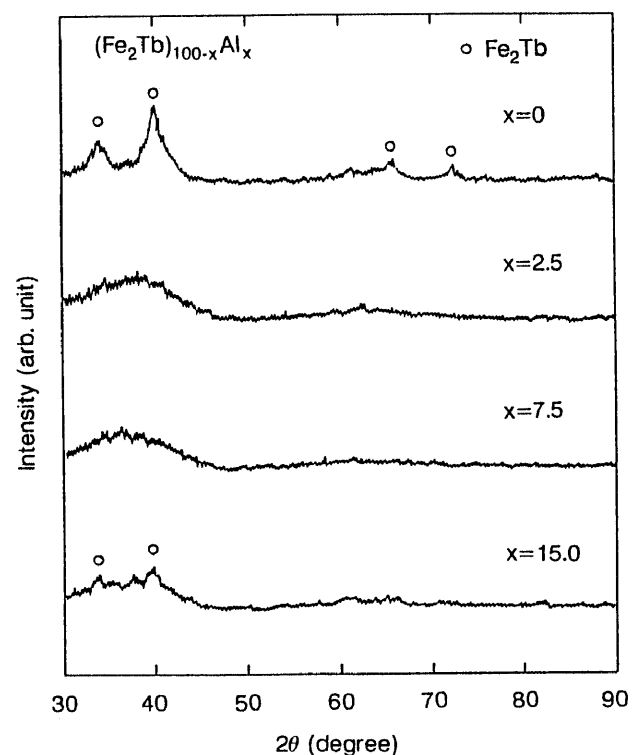


Fig. 2. X-ray diffraction patterns of rapidly solidified $(\text{Fe}_2\text{Tb})_{100-x}\text{Al}_x$ ($x=0, 2.5, 7.5$ and 15 at%) alloys.

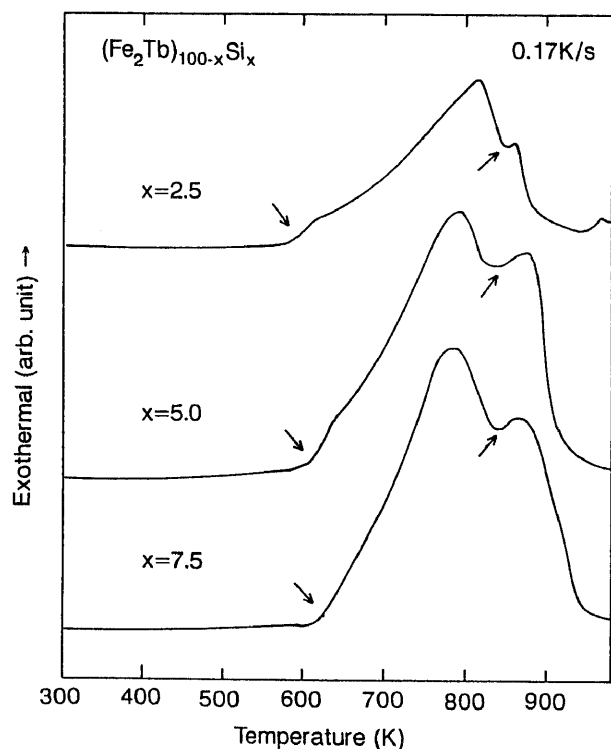


Fig. 3. DSC curves of amorphous $(\text{Fe}_2\text{Tb})_{100-x}\text{Si}_x$ ($x=0, 2.5$ and 7.5 at%) alloys.

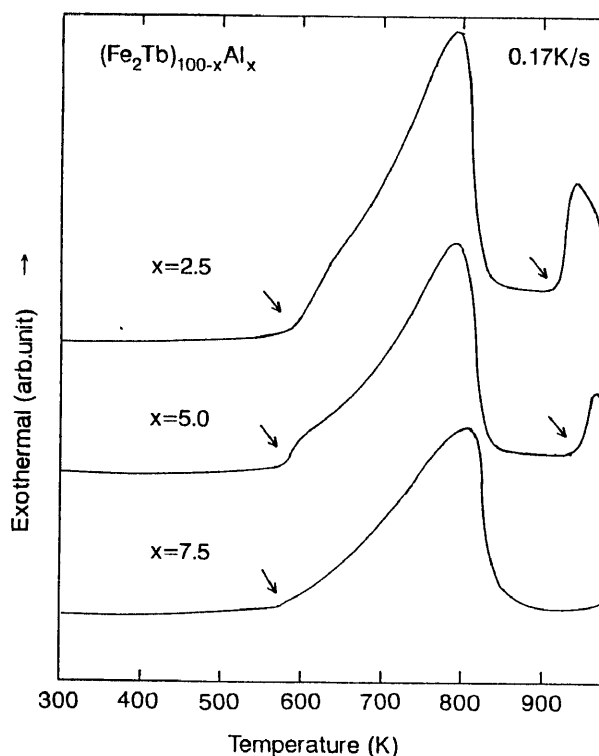


Fig. 4. DSC curves of amorphous $(\text{Fe}_2\text{Tb})_{100-x}\text{Al}_x$ ($x=0, 2.5$ and 7.5 at%) alloys.

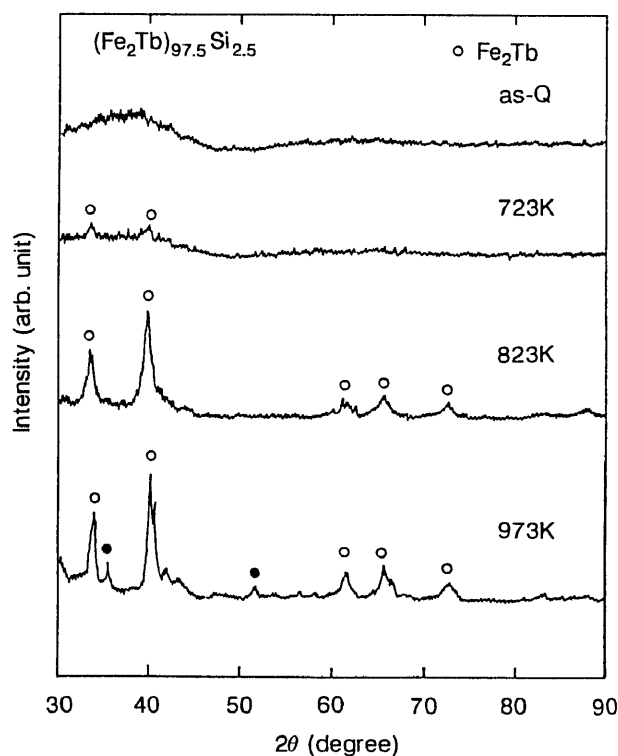


Fig. 5. X-ray diffraction patterns of an amorphous $(\text{Fe}_2\text{Tb})_{97.5}\text{Si}_{2.5}$ alloy annealed for 3.6 ks at 723, 823 and 973 K.

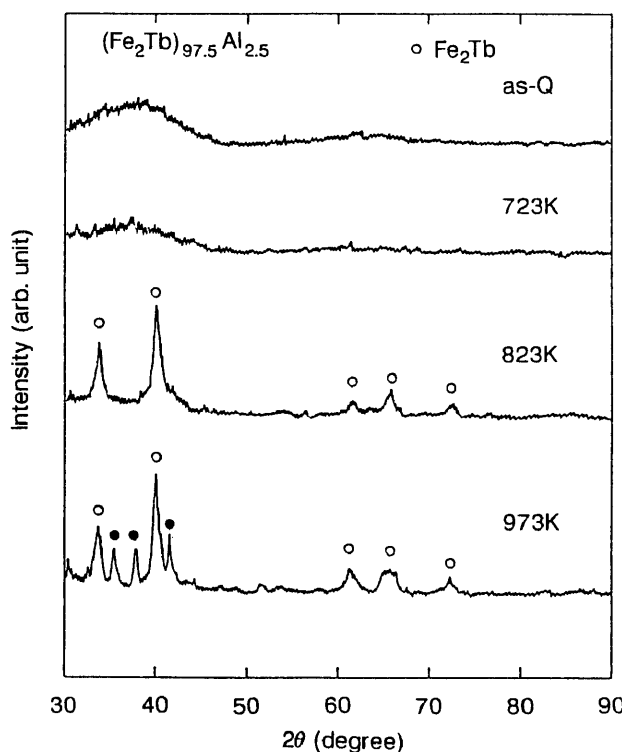


Fig. 6. X-ray diffraction patterns of an amorphous $(\text{Fe}_2\text{Tb})_{97.5}\text{Al}_{2.5}$ alloy annealed for 3.6 ks at 723, 823 and 973 K.

Considering that the Laves phase precipitates over the wide temperature interval of about 300 K, there is a high possibility of controlling the precipitation amount and particle size of the Laves phase in a coexistent state with the amorphous phase. Figure 7 shows bright-field electron

micrographs and selected-area diffraction patterns of the $(\text{Fe}_2\text{Tb})_{97.5}\text{Si}_{2.5}$ and $(\text{Fe}_2\text{Tb})_{97.5}\text{Al}_{2.5}$ alloys heated for 3.6 ks at 798 and 848 K, respectively. As identified in the diffraction patterns (b) and (d), all the diffraction rings are indexed to be the rhombohedral Laves phase with lattice parameters

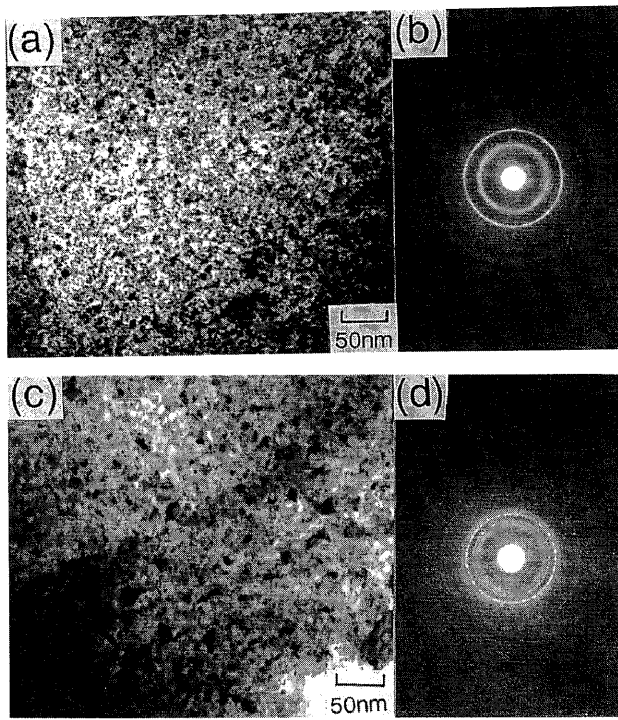


Fig. 7. Bright-field electron micrographs and selected-area diffraction patterns of $(\text{Fe}_2\text{Tb})_{97.5}\text{Si}_{2.5}$ (a and b) alloy annealed 3.6 ks at 798 K and $(\text{Fe}_2\text{Tb})_{97.5}\text{Al}_{2.5}$ (c and d) alloy annealed 3.6 ks at 843 K.

of $a=0.52$ nm and $c=1.28$ nm which agrees with those ($a=0.51896$ nm and $c=1.28214$ nm)⁸⁾ for Fe_2Tb . Thus, the Laves phase precipitates as fine isolated particles with a particle size of about 5 nm for the Fe-Tb-Si alloy and 17

nm for the Fe-Tb-Al alloy. This nanocrystalline structure indicates that the precipitation takes place through homogeneous nucleation and growth mechanism. Considering that these nanoscale Laves particles appear to be in an isolated state, these particles seem to be surrounded by the remaining amorphous phase. The residual existence of the amorphous phase is presumed to suppress the coarsening of the nanoscale Laves particles. Accordingly, it is said that the formation of the amorphous phase by the addition of a small amount of Al or Si into Fe_2Tb enables the fabrication of the Laves aggregates with nanoscale grain size which are not obtained by conventional preparation processes.

Figures 8 and 9 show the changes in the coercivity (H_c), magnetization at a field of 1440 kA/m (σ_{1440}) and magnetostriction at a field of 240 kA/m (λ_{240}) as a function of annealing temperature for the amorphous $(\text{Fe}_2\text{Tb})_{97.5}\text{Si}_{2.5}$ and $(\text{Fe}_2\text{Tb})_{97.5}\text{Al}_{2.5}$ alloys. It is seen that the precipitation of the Laves phase causes the increase in H_c , σ_{1440} and λ_{240} as compared with those for the amorphous single phase, followed by a maximum of σ_{1440} and λ_{240} and a minimum of H_c in the vicinity of 850 K which is just below the precipitation temperature of the second compound phase, and then the increase in H_c and the decrease in σ_{1440} and λ_{240} by the precipitation of the second compound phase. Thus, the best combination of the lowest H_c value and the highest σ_{1440} and λ_{240} values is obtained for the metastable phase consisting of the nanoscale Laves particles surrounded by the remaining amorphous phase. The best values of H_c , σ_{1440} and λ_{240} in the present annealing treatment are 175 kA/m, 61 emu/g and 985×10^{-6} for the Fe-Tb-Si alloy and 136 kA/m, 60 emu/g and 895×10^{-6} for the Fe-Tb-Al alloy. In order to examine the ease of the increase in λ with increasing applied magnetic field, the λ value as a function of

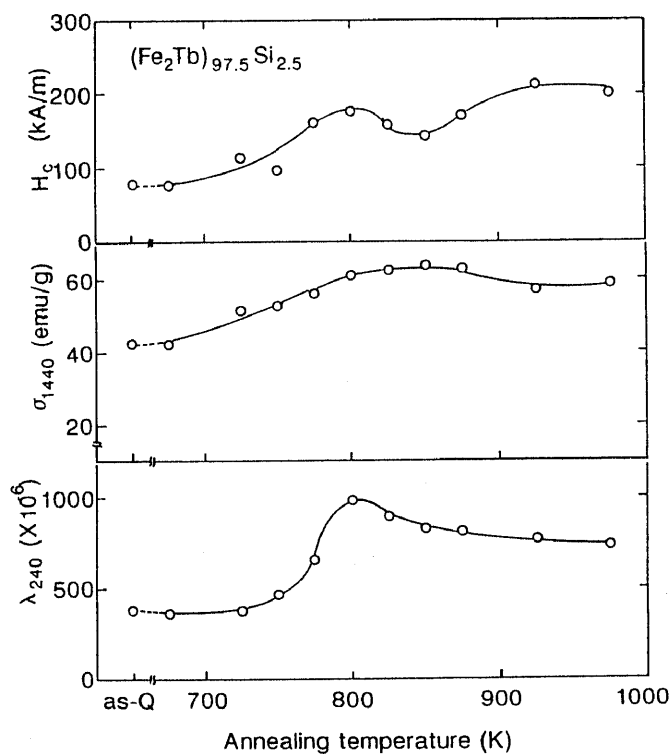


Fig. 8. Changes in H_c , σ_{1440} and λ_{240} with T_a for an amorphous $(\text{Fe}_2\text{Tb})_{97.5}\text{Si}_{2.5}$ alloy.

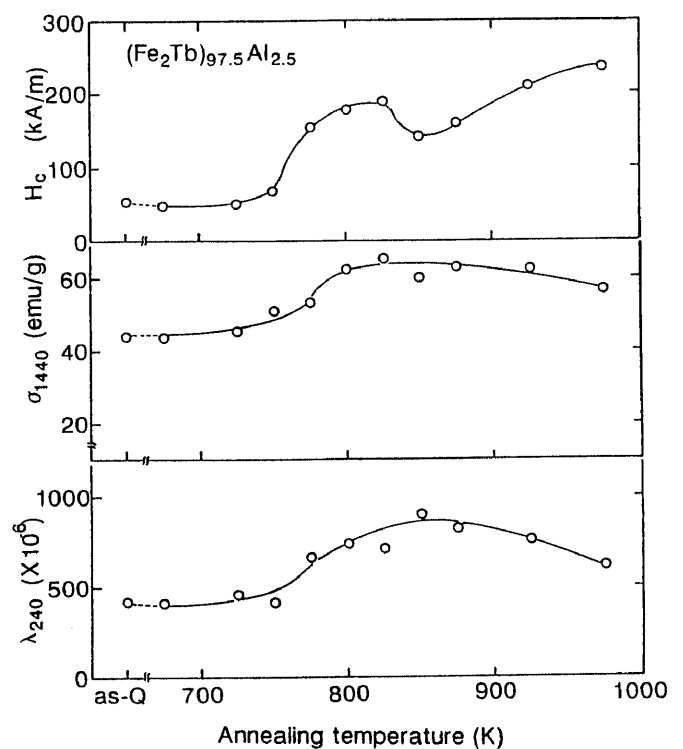


Fig. 9. Changes in H_c , σ_{1440} and λ_{240} with T_a for an amorphous $(\text{Fe}_2\text{Tb})_{97.5}\text{Al}_{2.5}$ alloy.

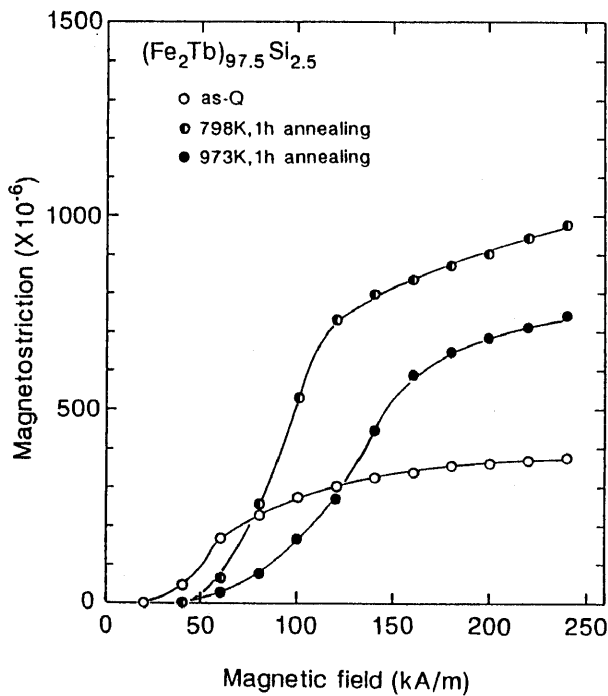


Fig. 10. Magnetostriction (λ) as a function of magnetic field for an amorphous $(\text{Fe}_2\text{Tb})_{97.5}\text{Si}_{2.5}$ alloy in as-quenched and annealed for 3.6 ks at 798 and 973 K.

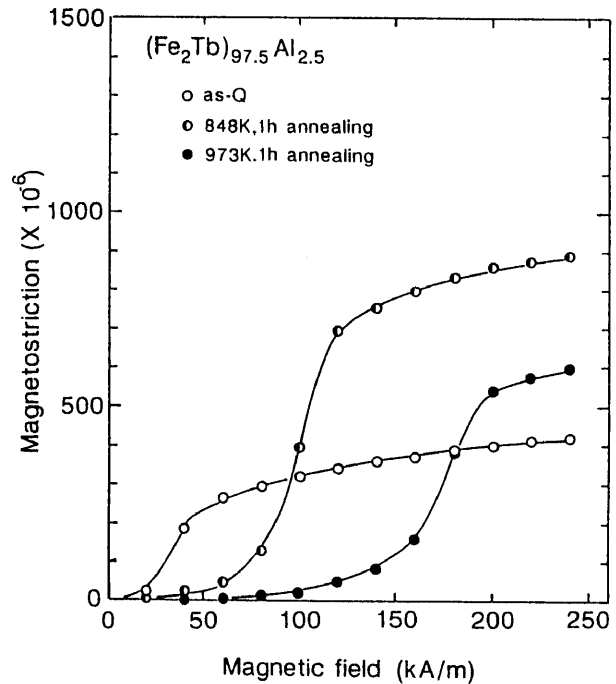


Fig. 11. Magnetostriction (λ) as a function of magnetic field for an amorphous $(\text{Fe}_2\text{Tb})_{97.5}\text{Al}_{2.5}$ alloy in as-quenched and annealed for 3.6 ks at 848 and 973 K.

magnetic field is plotted in Fig. 10 for the $(\text{Fe}_2\text{Tb})_{97.5}\text{Si}_{2.5}$ alloy and in Fig. 11 for the $(\text{Fe}_2\text{Tb})_{97.5}\text{Al}_{2.5}$ alloy with the three different structural states of amorphous single phase, mixed nanocrystalline Laves plus amorphous phases and mixed Laves plus compound phases. A similar tendency is seen for both the alloys. That is, the increase in λ in a low applied magnetic field is the largest for the amorphous samples, followed by the nanocrystalline Laves and amorphous phases and then the Laves and compound phases. However, the maximum λ value decreases in the order of the nanocrystalline Laves and amorphous phases > the mixed Laves and compound phases > the amorphous phase. From the comparison of the $\lambda(H)$ behavior among the three structural states, one can notice that the nanocrystalline Laves aggregates exhibit the best combined properties of a rather rapid increase in λ in a low applied field and the largest λ value in a high magnetic field.

Figure 12 shows the gradient of λ at an applied field of 100 kA/m in the relation between λ and H as a function of annealing temperature for the $(\text{Fe}_2\text{Tb})_{97.5}\text{M}_{2.5}$ ($\text{M}=\text{Si}$ or Al) alloys consisting mainly of the nanoscale Laves structure. The largest value of λ/H is obtained at the annealing temperature where the λ_{240} has the maximum value. Thus, the variation of λ with applied field for the Laves phase is the greatest in the nanoscale grain structure, indicating the effectiveness of the nanostructure control for the Laves phase in the development of a favorable magnetostrictive material.

The data of magnetostriction shown in Figs. 8 to 12 were obtained only from the Fe_2Tb alloys containing Al or Si of 2.5 at%. Consequently, we further examined the change in λ_{240} as a function of Al or Si content for the $(\text{Fe}_2\text{Tb})_{100-x}\text{Al}_x$ and $(\text{Fe}_2\text{Tb})_{100-x}\text{Si}_x$ alloys with the amorphous or nanocrystalline Laves phases. As shown in Fig. 13, λ_{240} of both

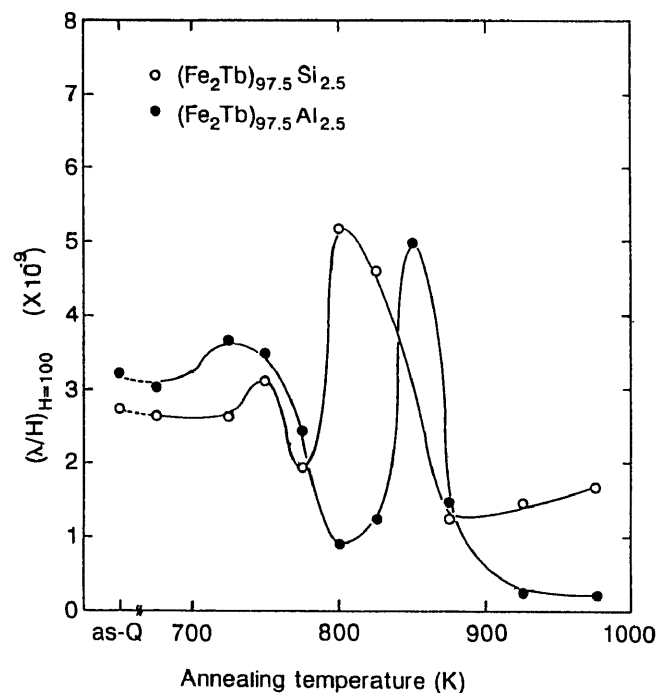


Fig. 12. Change in the increase in λ with increasing H at a field of 100 kA/m, $(\lambda/H)_{H=100}$, as a function of T_a for amorphous $(\text{Fe}_2\text{Tb})_{97.5}\text{M}_{2.5}$ ($\text{M}=\text{Si}$ or Al) alloys.

phases decreases significantly with increasing Al or Si content. This change indicates that the increase in the amount of the third element to Fe_2Tb is harmful for the achievement of large magnetostriction even in the nanocrystalline Laves and amorphous phases.

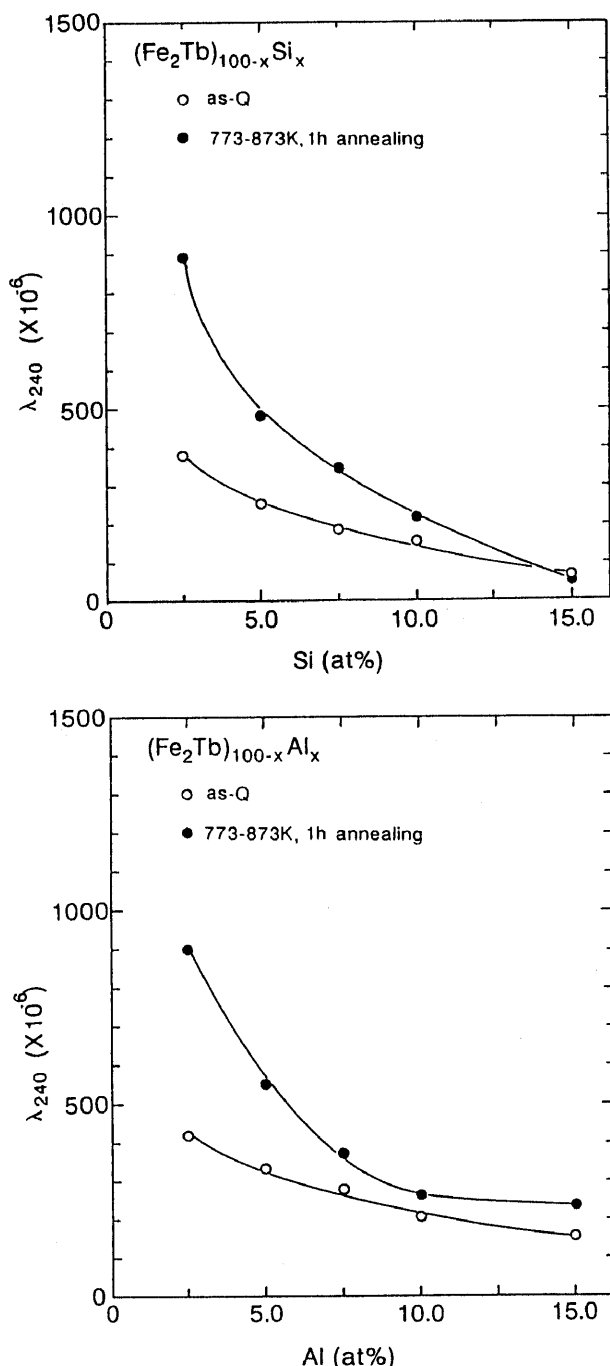


Fig. 13. Change in the magnetostriction (λ_{240}) at a field of 240 kA/m with Al or Si content for amorphous $(\text{Fe}_2\text{Tb})_{97.5-x}\text{M}_x$ ($\text{M}=\text{Al}$ or Si) alloys in as-quenched state and annealed for 3.6 ks at optimum temperatures.

4. Discussion

It is generally known that no amorphous single phase is formed in Fe-Tb, Fe-Al and Tb-Al binary systems by melt spinning. It is therefore important to discuss the reason for the significant effect of the addition of Si or Al on the increase in the glass-forming ability. It has recently been reported⁹⁻¹¹ that very wide glass formation ranges as well as very large glass-forming ability are obtained in Ln-Al-TM (Ln=lanthanide metal including Tb, TM=transition metal including Fe) ternary system by rapid solidification.

The formation of the ternary amorphous alloys with large glass-forming ability in the Ln-Al-TM system has been interpreted¹¹ to be due to the combination effect of the following three factors; (1) appropriate atomic size effect in which the three constituent elements have significantly different atomic sizes which can be divided into larger, intermediate and smaller sizes, (2) the necessity of long-range redistribution of the constituent elements for crystallization, and (3) rather large negative heat of mixing among the constituent elements. It is reasonable to consider that the same concept is applied to the interpretation of the formation of the amorphous phase in the ternary Fe-Tb-Al system.

However, the same concept cannot be applied to the glass formation in the Fe-Tb-Si system because the difference in the atomic size is not significant between Si and Fe and Si belongs to be a metalloid element. However, one can remind of the formation of amorphous alloys in Tb-Si binary system¹², though no amorphous phase is formed in Fe-Si and Fe-Tb binary systems. That is, it may be interpreted that the glass formation range in the binary Tb-Si system is extended to the Tb-Si-Fe ternary alloys because the Tb-Fe and Fe-Si pairs also have large negative heats of mixing.

Secondarily, we shall discuss the reason why the Laves compound in the Fe-Tb-Al and Fe-Tb-Si systems precipitates over the extremely wide temperature interval of about 300 K. This result is in good contrast to the result that an amorphous Fe_2Tb phase prepared by sputtering crystallizes in a rather narrow temperature interval below 150 K. It is therefore said that the addition of a small amount of Al or Si has a significant effect on the extension of the temperature interval where the Fe_2Tb phase precipitates. It is pointed out in Figs. 5 and 6 that the second compound which precipitates from the remaining amorphous phase contains a large amount of Al or Si. This result indicates that the additional Si or Al element has been concentrated to the remaining amorphous phase. That is, the progress of the primary crystallization stage requires the redistribution of Si or Al from the Laves phase to the remaining amorphous phase. The redistribution of Si or Al is thought to cause the retardation of the precipitation of the Laves phase, leading to the appearance of the precipitation temperature interval reaching about 300 K. The dominant role of Al or Si in the extension of the precipitation temperature range also implies that the refinement of the Laves phase into the nanoscale particle size is attributed to the dissolution of Al or Si into the amorphous phase. The dissolution of Al or Si into the Fe_2Tb Laves phase is presumed to be very difficult because of its strict stoichiometricity¹³. Therefore, the growth of the Laves phase requires the redistribution of Al or Si into the remaining amorphous phase, leading to the increase in the solute content in the remaining amorphous phase. As a result, the thermal stability of the amorphous phase increases and the amorphous phase exists up to the high temperature of about 850 K. The residual existence of the amorphous phase up to the high temperature suppresses the progress of the growth and coalescence of the primary Laves particles, leading to the appearance of the extremely wide temperature interval for the precipitation of the Laves phase.

Thus, the finding that the addition of a small amount of Si

or Al into the Laves Fe_2Tb alloy causes the increase in the glass-forming ability as well as the formation of the nano-crystalline Laves aggregates through the necessity of the long-range redistribution of Al or Si is quite significant for subsequent interpretation of the crystallization behavior of amorphous alloys with alloy components near the Laves phase. The alloy design along this new concept is expected to enable the appearance of a new type of high magnetostrictive alloys with high sensitivity in a low magnetic field through the formation of further finely mixed Laves and amorphous phases.

5. Summary

The glass-formation of melt-spun $(\text{Fe}_2\text{Tb})_{100-x}\text{M}_x$ ($\text{M}=\text{Si}$ or Al) alloys, the crystallization behavior of the resulting amorphous alloys and the magnetic properties of the amorphous and crystallized alloys were examined with the aim of developing a high magnetostrictive alloy with high sensitivity in a low magnetic field through the grain size refinement of the Laves Fe_2Tb phase. The results obtained are summarized as follows.

(1) The addition of 2.5 %Si or Al to Fe_2Tb causes the formation of an amorphous single phase and the glass formation ranges extend up to 15 %Si or Al which is the maximum content in the present study.

(2) The $(\text{Fe}_2\text{Tb})_{97.5}\text{M}_{2.5}$ ($\text{M}=\text{Si}$ or Al) amorphous alloys crystallize through two stages of $\text{Am} \rightarrow \text{Laves } \text{Fe}_2\text{Tb} + \text{Am} \rightarrow \text{Fe}_2\text{Tb} + \text{unknown compound containing Si or Al}$. The temperature interval for the precipitation of the primary Fe_2Tb phase is as large as about 300 K and the particle size is as small as about 20 nm. The nanoscale Fe_2Tb particles are surrounded by the remaining amorphous phase with Si or Al concentration higher than the nominal concentration.

(3) The finely mixed structure consisting of nanoscale Fe_2Tb particles and amorphous phase exhibits good combined magnetic properties of high σ_{1440} , low H_c , high λ_s and high λ/H and their values are 60 emu/g, 136 kA/m, 895×10^{-6} and 5.0×10^{-9} , respectively, for $(\text{Fe}_2\text{Tb})_{97.5}\text{Al}_{2.5}$ and 61 emu/g, 175 kA/m, 985×10^{-6} and 5.3×10^{-9} , respectively,

for $(\text{Fe}_2\text{Tb})_{97.5}\text{Si}_{2.5}$. These magnetic properties become worse by the structural change into the mixed structure of Fe_2Tb and unknown compounds.

(4) The absence of the solubility limit of Al or Si into Fe_2Tb and hence the necessity of the long-range redistribution of Al or Si to the remaining amorphous phase are presumed to cause the large temperature interval for the precipitation of the Fe_2Tb phase, leading to the finely mixed structure consisting of nanoscale Fe_2Tb particles surrounded by the remaining amorphous phase.

- 1) T. Masumoto, H.M. Kimura, A. Inoue and Y. Waseda, *Mater. Sci. Eng.*, **23**(1976), 141.
- 2) Y. Yoshizawa, S. Oguma and K. Yamauchi, *J. Appl. Phys.*, **64**(1988), 6044.
- 3) N. Hasegawa and M. Saito, *J. Magn. Soc. Japan*, **14**(1990), 313.
- 4) K. Suzuki, A. Makino, N. Kataoka, A. Inoue and T. Masumoto, *Mater. Trans., JIM*, **32**(1991), 93.
- 5) K. Suzuki, A. Makino, A. Inoue and T. Masumoto, *J. Appl. Phys.*, **70**(1991), 6232.
- 6) A.E. Clark, *Ferromagnetic Materials*, Ed. by E.P. Wohlfarth, Vol.1, North-Holland, Amsterdam, (1980), p.531.
- 7) Y. Tanaka, A. Inoue and T. Masumoto, unpublished research (1991).
- 8) A.E. Dwight and C.W. Kimball, *Acta Crystallogr.*, **B30**(1974), 2791.
- 9) A. Inoue, T. Zhang and T. Masumoto, *Mater. Trans., JIM*, **30**(1989), 965.
- 10) A. Inoue, H. Yamaguchi, T. Zhang and T. Masumoto, *Mater. Trans., JIM*, **31**(1990), 104.
- 11) A. Inoue, T. Zhang and T. Masumoto, *J. Non-Cryst. Solids*, 156-158(1993), 473.
- 12) K. Matsuzaki, Master Thesis, Tohoku University (1984).
- 13) M.P. Dariel, J.P. Holthuis, M.R. Pickus, *J. Less-Common Met.*, **45**(1976), 91.